# Effect of systematics in the T2HK, T2HKK, and DUNE experiments

Monojit Ghosh[*] and Osamu Yasuda[†]

*Department of Physics, Tokyo Metropolitan University, Hachioji, Tokyo 192-0397, Japan*

(Received 2 March 2017; published 10 July 2017)

T2HK and T2HKK are the proposed extensions of the T2K experiments in Japan and DUNE is the future long-baseline program of Fermilab. These three experiments will use extremely high beam power and large detector volumes to observe neutrino oscillation. Because of the large statistics, these experiments will be highly sensitive to systematics. Thus a small change in the systematics can cause a significant change in their sensitivities. To understand this, we do a comparative study of T2HK, T2HKK, and DUNE with respect to their systematic errors. Specifically we study the effect of the systematics in the determination of neutrino mass hierarchy, octant of the mixing angle $\theta_{23}$, and $\delta_{CP}$ in the standard three-flavor scenario, and we also analyze the role of systematic uncertainties in constraining the parameters of the nonstandard interactions in neutrino propagation. Taking the overall systematics for signal and background normalization, we quantify how the sensitivities of these experiments change if the systematics are varied from 1% to 7%.

DOI: 10.1103/PhysRevD.96.013001

## I. INTRODUCTION

The phenomenon of neutrino oscillation suggests that neutrinos have mass and mixing. In the standard three-flavor scenario, neutrino oscillations are described by three mixing angles, i.e., $\theta_{12}$, $\theta_{13}$, $\theta_{23}$; two mass-squared differences, i.e., $\Delta m^2_{21}$, $\Delta m^2_{31}$; and one Dirac-type $CP$ phase, i.e., $\delta_{CP}$. Among these six parameters at this moment the unknowns are (i) the neutrino mass hierarchy, i.e., normal hierarchy (NH: $\Delta m^2_{31} > 0$) or inverted hierarchy (IH: $\Delta m^2_{31} < 0$); (ii) the octant of the mixing angle $\theta_{23}$, i.e., lower octant (LO: $\theta_{23} < 45°$) or higher octant (HO: $\theta_{23} > 45°$); and (iii) the $CP$ phase $\delta_{CP}$. As the appearance channel probability, which gives the transition of $\nu_\mu \to \nu_e$, depends on these three unknowns, in principle, the accelerator-based long-baseline experiments can determine them by studying the electron events at the far detector. Currently running such kinds of experiments are T2K [1] and NO$\nu$A [2]. The recent results of T2K show a mild preference for the normal hierarchy, $\theta_{23} = 45°$ and $\delta_{CP} = -90°$. On the other hand, the current NO$\nu$A results are in accordance with T2K regarding the fit to the hierarchy and $\delta_{CP}$, but the current NO$\nu$A results exclude maximal mixing at $2.6\sigma$ [3]. Note that at this moment the statistical significance of these hints is very weak and one needs further data to establish the true nature of these parameters on a firm footing.

Due to comparatively shorter baselines, low beam power and small detector sizes, the sensitivities of T2K and NO$\nu$A are limited. The shorter baselines of T2K and NO$\nu$A restrict them to have sensitivity only in the favorable parameter space [4,5]. These experiments also suffer from parameter degeneracy due to a lesser matter effect [6,7]. Even in the favorable parameter space, these experiments cannot have much sensitivity for their low statistics [8–15]. Thus it is the job of the future high statistics long-baseline experiments to determine the remaining unknowns in the neutrino oscillation in a conclusive manner. The examples of such experiments are T2HK [16], T2HKK [17], and DUNE [18]. Due to the smaller baseline, T2HK will not have much hierarchy sensitivity in the unfavorable parameter space, but it can have excellent sensitivity in the favorable parameter space [19,20]. Thus if nature chooses a favorable value of the unknown parameters, then T2HK will be sufficient to determine them at a conclusive level. Apart from establishing the true nature of the unknown parameters in the standard three-neutrino picture, these future long-baseline experiments can also probe different new physics scenarios like nonstandard interactions (NSI) in neutrino propagation [21–25]. NSI has caught a lot of attention particularly because Ref. [26] pointed out that there is a tension between the mass-squared difference deduced from the solar neutrino observations and the one from the KamLAND experiment, and that the tension can be resolved by introducing the flavor-dependent NSI in neutrino propagation. Recent studies of NSI in neutrino propagation for the long-baseline experiments can be found in [27–49]. All these experiments mentioned above will use high beam power and large detectors. Thus it is easy to understand that these experiments will be highly sensitive to the effect of the systematics. The systematic errors in the long-baseline experiments arise mainly from the uncertainties related to fluxes and cross sections. Studies of different sources of systematic uncertainties affecting the measurement of neutrino oscillation parameters can be found in Refs. [50–56]. Due to the large number of event samples in the far detector, a slight improvement in these systematic errors can improve the sensitivity of these experiments

[*]mghosh@phys.se.tmu.ac.jp
[†]yasuda@phys.se.tmu.ac.jp

 

significantly. Thus it will be quite intriguing to see how the sensitivity of these experiments to determine hierarchy, octant, and $CP$ violation in the standard three-flavor scenario, as well as to constrain the NSI parameters assuming the existence of NSI in nature, depends on the systematic error. Adopting a very simplistic treatment,[1] we express the systematic errors in terms of an overall signal and background normalization and present our results as a function of the systematics for T2HK, T2HKK, and DUNE.

The plan of the paper goes as follows. In the next section we will discuss the experimental specification and simulation details. We will also mention our treatment of the systematics in that section. In Sec. III we will present the hierarchy, octant, and $CP$ violation sensitivity of the three experiments as a function of the systematic error in the standard three-flavor scenario. In Sec. IV, we give our results corresponding to nonstandard interactions for different values of the systematic errors. Finally in Sec. V we will summarize our results and give our conclusions.

## II. EXPERIMENTAL AND SIMULATION DETAILS

For our analysis we assume that under the T2HK project the two water Čerenkov detector tanks, each of fiducial mass 187 kt, will be placed at the Kamioka site and that for the T2HKK experiment one of the tanks will be at the Kamioka and the other in Korea. The neutrino source for both setups is J-PARC and the baseline lengths are 295 km for Kamioka and 1100 km for Korea. Depending on the locations in Korea, the beam from J-PARC will reach the detector at different off-axis angles. For the present work we consider the flux options of 2.5°, 2.0°, and 1.5°. The off-axis angle for the Kamioka site is 2.5°. We have considered a beam power of 1.3 MW with a total exposure of $27 \times 10^{21}$ protons on target (pot). This corresponds to a 10 year running of both experiments. Following the T2HKK report, we have divided this runtime in 1∶3 for neutrino and antineutrino modes to compensate the lower antineutrino cross sections [17]. We have matched our events with the latest T2HKK report and our results are consistent with their sensitivity [17]. For DUNE we use a beam power of 1.2 MW, leading to a total exposure of $10 \times 10^{21}$ pot. We assume a liquid argon detector of fiducial mass 40 kt. The baseline for DUNE is 1300 km. We take the ratio to the neutrino and antineutrino run as 1∶1. Our simulation results of DUNE are consistent with [18]. We have used the GLoBES [58,59] and MonteCUBES [60] softwares to simulate all of the above experiments.

We estimate the sensitivity of each experiment in terms of $\chi^2$. We calculate the statistical $\chi^2$ by comparing the true events $N^{\rm true}$ and test events $N^{\rm test}$ using the following Poisson formula:

$$\chi^2_{\rm stat} = \sum_i 2\left[N_i^{\rm test} - N_i^{\rm true} - N_i^{\rm true}\log\left(\frac{N_i^{\rm test}}{N_i^{\rm true}}\right)\right], \quad (1)$$

where the index $i$ corresponds to the number of energy bins. To incorporate the effect of the systematics, we deviate the test events by

$$N_i^{\rm test} \to N_i^{\rm test}\left(1 + \sum_k c_i^k \xi_k\right), \quad (2)$$

where $c_i^k$ is the $1\sigma$ systematic error corresponding to the pull variable $\xi_k$. Here the index $k$ stands for the number of pull variables. After modifying the events, the combined statistical and systematic $\chi^2$ is calculated as

$$\chi^2_{\rm stat+sys} = \chi^2_{\rm stat} + \sum_k \xi_k^2. \quad (3)$$

The final $\chi^2$ is obtained by varying $\xi_k$ from $-3$ to $+3$, corresponding to their $3\sigma$ ranges and minimizing over $\xi_k$, i.e.,

$$\chi^2 = \min\{\xi_k\}[\chi^2_{\rm stat+sys}]. \quad (4)$$

For our analysis of the long-baseline experiments we take four pull variables. These variables are (i) signal normalization error, (ii) signal tilt error, (iii) background normalization error, and (iv) background tilt error. The normalization error affects the scaling of the events, whereas the tilt error or the energy calibration error affects the energy dependence of the events. The tilt error is incorporated in our analysis by varying the test events in the following way:

$$N_i^{\rm test} \to N_i^{\rm test}\left(1 + \sum_k c_i^k \xi_k \frac{E_i - E_{\rm av}}{E_{\rm max} - E_{\rm min}}\right), \quad (5)$$

where $E_i$ is the energy in the $i$th bin, $E_{\rm min}$ is the lower limit of the full energy range, $E_{\rm max}$ is the higher limit of the full energy range, and $E_{\rm av} = 1/2(E_{\rm min} + E_{\rm max})$. For simplicity we have assumed that the systematic errors for the neutrino mode and the antineutrino mode are the same. For our simulation we have fixed the tilt error to a constant value, which is 10% for T2HK/T2HKK and 2.5% for DUNE, corresponding to all the channels. We do not vary these tilt pull variables in our analysis.[2] On the other hand, the signal and background normalization errors for T2HK, T2HKK, and DUNE are considered as variables in our analysis. We have taken them to be the same for both the appearance and disappearance channel. Thus a systematic uncertainty of $x$%

[1] A detailed analysis of the systematics in long-baseline experiments can be found in [57].

[2] Note that the values for the tilt variables are chosen such that our simulation results match with the sensitivities as reported in the collaboration papers. Thus a variation of the pull variables can also affect the results significantly.

implies a signal and a background normalization error of $x$% for both the appearance and disappearance channel.

Note that our treatment of the systematics is quite simplistic. In the T2HKK report [17], they have considered a total of eight pull variables and the values are listed in Table V of the report. In the DUNE report the systematic uncertainty is taken as a 2% normalization error in the appearance channel with respect to the normalization determined from the disappearance signal, assumed to be known with 5% uncertainty [18].

## III. RESULTS FOR STANDARD THREE-FLAVOR CASE

In this section we will present the $CP$ violation, hierarchy, and octant sensitivity of T2HK, T2HKK, and DUNE as a function of the systematic errors. In generating these results the parameters $\theta_{12}$, $\theta_{13}$, $\Delta m^2_{21}$, and $\Delta m^2_{31}$ are kept fixed close to their best values as obtained in global fits [61–63] in both the true and test spectrum. To ensure that the wrong hierarchy minimum occurs at a correct value, we have used the effective formula $\Delta m^2_{\mu\mu}$ given by

$$\Delta m^2_{31} = \Delta m^2_{\mu\mu} + (\cos^2\theta_{12} - \cos\delta_{CP} \sin\theta_{13} \sin 2\theta_{12} \tan\theta_{23})\Delta m^2_{21}. \quad (6)$$

This is because in the three-flavor scenario, the hierarchy degeneracy does not correspond to $P_{\mu\mu}(\Delta m^2_{31}) = P_{\mu\mu}(-\Delta m^2_{31})$ but it occurs for $P_{\mu\mu}(\Delta m^2_{\mu\mu}) = P_{\mu\mu}(-\Delta m^2_{\mu\mu})$ [64,65]. For the $CP$ violation study, we have taken the true $\theta_{23} = 45°$ and marginalized over $\theta_{23}$, $\delta_{CP}$, and hierarchy in the test. For hierarchy sensitivity, the true value of $\theta_{23}$ is 45° and the true value of $\delta_{CP}$ is $\pm 90°$. In this case we have marginalized over $\theta_{23}$ and $\delta_{CP}$ in the test. For octant sensitivity, the true value of $\theta_{23}$ is assumed to be 42° for the lower octant and 48° for the higher octant. These values of $\theta_{23}$ are the closest to the best-fit values as obtained by the global fits. The true value of $\delta_{CP}$ is $-90°$. For octant sensitivity, we have marginalized over $\delta_{CP}$ and hierarchy in the test.

### A. *CP* violation sensitivity

$CP$ violation (CPV) discovery potential of an experiment is defined by its capability to distinguish a true value of $\delta_{CP}$ other than 0° or 180°. In Fig. 1, we have plotted the fraction of the true $\delta_{CP}$ for which CPV can be discovered at $5\sigma$ vs systematics. The left panel is for the normal hierarchy and the right panel is for the inverted hierarchy. From the figures we see that the CPV coverage of DUNE falls from 50% (55%) to 0% (15%) when the systematics is varied from 1% to 7% for NH (IH). For T2HK, the numbers are 50% (50%) to 5% (10%) if the hierarchy is unknown and 75% (80%) to 15% (20%) if hierarchy is known for NH (IH). For the 2.5° off-axis configuration of T2HKK, the sensitivity falls from 65% to 45% for both hierarchies. For the 2.0° (1.5°) off-axis configuration it falls from 70% (75%) to 50% (50%) in both NH and IH. Thus from these numbers we understand that the dependence of the sensitivity of T2HK on the systematic errors is stronger than that of T2HKK. This can be understood in the following way. For T2HK the baseline length is small compared to that of T2HKK. Now as the flux drops in proportion to $1/L^2$ (where $L$ is the baseline length) T2HK has much larger event samples at the detector than the T2HKK experiment does and thus it is more sensitive to the systematic errors. From the figure we also see that when the hierarchy is unknown, then the solid curve (T2HK) always lies below the T2HKK curves. This is because of the presence of degeneracies which restrict the CPV sensitivity of T2HK. However, if the hierarchy is known then we see that the CPV discovery sensitivity of T2HK is better than the 2.5° configuration of T2HKK if the systematics is less than 4%

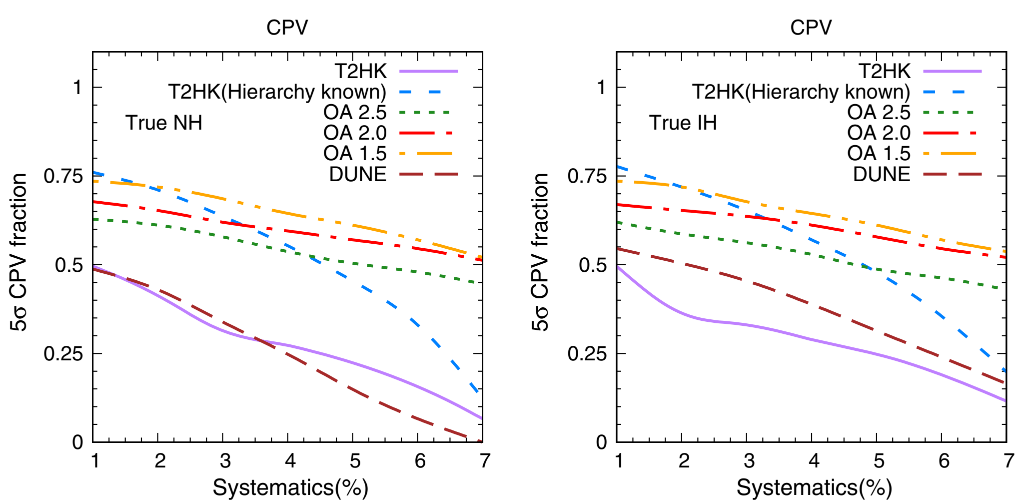


FIG. 1. Fraction of the true $\delta_{CP}$ for which $CP$ violation can be discovered for $5\sigma$ vs systematics. In all the panels the true $\theta_{23}$ is 45°. The left panel is for NH and the right panel is for IH.

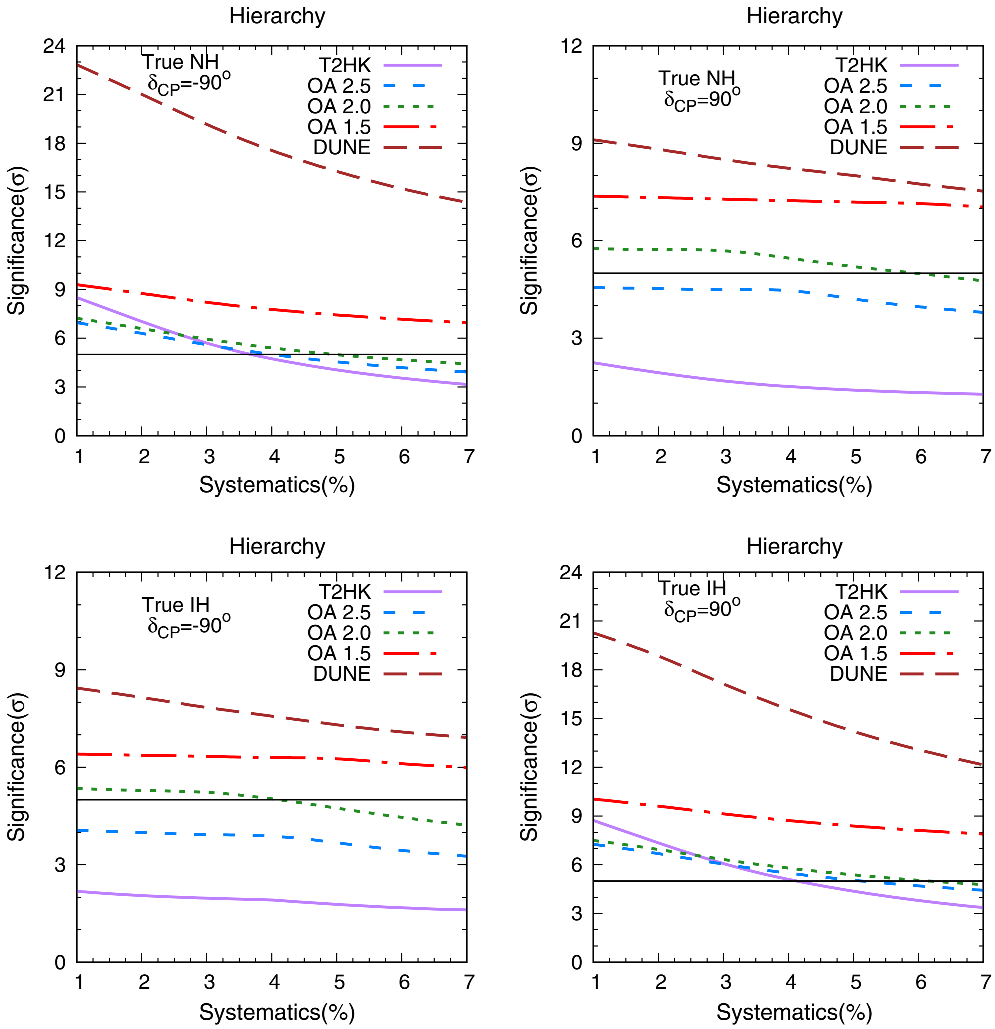


FIG. 2. Hierarchy sensitivity vs systematics. In all the panels the true value of $\theta_{23}$ is 45°. The true $\delta_{CP}$ is −90° for the left column and +90° for the right column. The upper row corresponds to the true NH and the lower row corresponds to the true IH.

and better than all three configurations of T2HKK if the systematics is less than 1% for both hierarchies. This is one of the most important findings of our work. From the figures we also note that the CPV discovery potential of DUNE is comparable to T2HK in NH and slightly higher than T2HK in IH for all the values of systematic errors.

### B. Hierarchy sensitivity

The hierarchy sensitivity of an experiment is defined by its capability to rule out the wrong hierarchy solutions. In Fig. 2, we have plotted the hierarchy sensitivity of T2HK, T2HKK, and DUNE vs the systematic error. The top row is for the normal hierarchy and the bottom row is for the inverted hierarchy. In each row the left panel is for $\delta_{CP} = -90°$ and the right panel is for $\delta_{CP} = 90°$. The horizontal thin solid line corresponds to $5\sigma$ C.L. For the determination of the hierarchy, the favorable combinations of $\delta_{CP}$ and hierarchy are {NH, −90°} and {IH, +90°}. These combinations are favorable in determination of the hierarchy because there is no degeneracy for these combinations. On the other hand, the other two combinations {NH, 90°} and {IH, −90°} are not favorable to determine the hierarchy because they suffer from degeneracy.

First let us discuss the hierarchy sensitivity for the unfavorable region (top right and bottom left panels). In these cases we see that all the curves are almost flat and do not vary much with respect to the systematics. This is because the sensitivity in the unfavorable parameter space is limited due to the existence of parameter degeneracy and hence the hierarchy sensitivity in the unfavorable parameter space is not dominated. From the plots we see that the sensitivity of DUNE is slightly better than the 1.5° off-axis configuration of T2HKK. The sensitivity of DUNE falls from $9\sigma$ to $7.5\sigma$ ($8.5\sigma$ to $7\sigma$) in NH (IH) as the systematics vary from 1% to 7%. For the T2HKK configuration of 1.5°, corresponding sensitivities are $7.5\sigma$ to $7\sigma$ ($6.5\sigma$ to $6\sigma$) for NH (IH). For the off-axis configurations 2.5° of T2HKK, the sensitivity falls from $4.5\sigma$ to $4\sigma$ ($4\sigma$ to $3\sigma$) in NH (IH). For the T2HKK configuration of 2.0° the

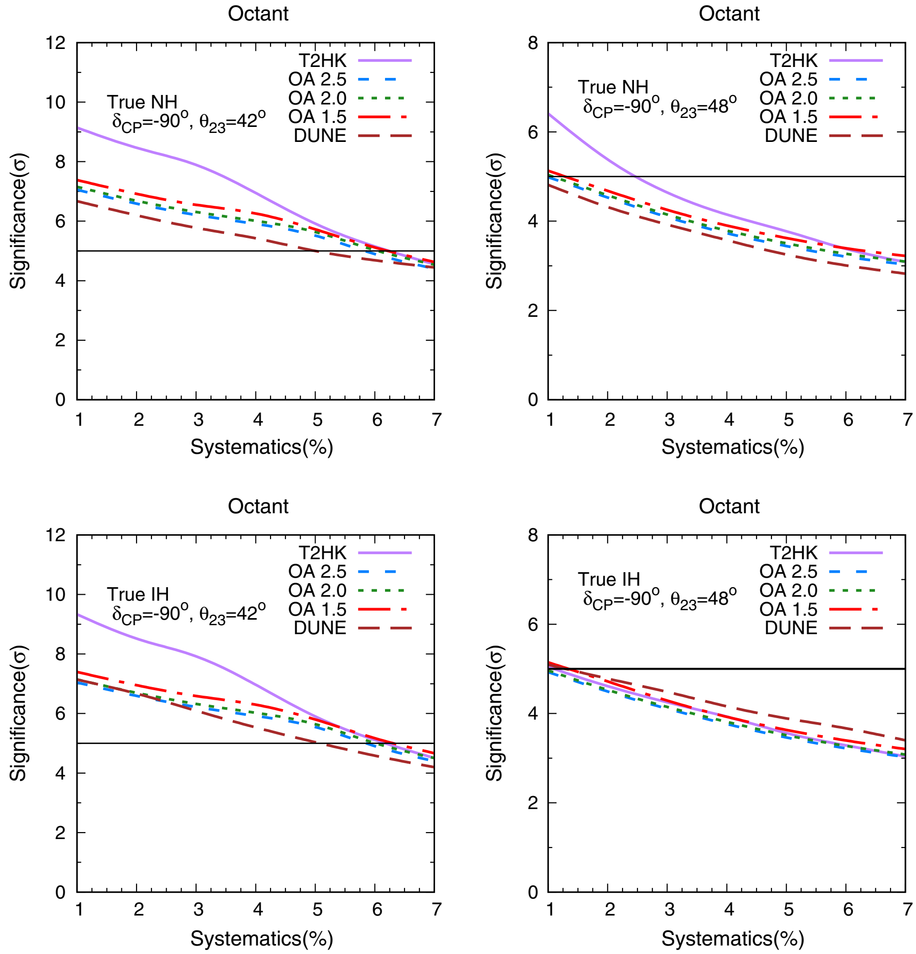


FIG. 3. Octant sensitivity vs systematics. The upper row corresponds to NH and the lower row corresponds to IH. Sensitivities are given for two values of $\theta_{23}$, i.e., 42° and 48° and for $\delta_{CP} = -90°$.

numbers are $6\sigma$ to $5\sigma$ ($5.5\sigma$ to $4\sigma$) for NH (IH). Here we find that the sensitivity of T2HK is the lowest for all the values of the systematics and it remains close to $2\sigma$ for both hierarchies.

For the favorable combinations (top left and bottom right panels) we see that the sensitivity of DUNE is maximal among all the setups for all the values of the systematics and the sensitivity falls from $23\sigma$ ($20\sigma$) to $14\sigma$ ($12\sigma$) for NH (IH) as the systematics varies from 1% to 7%. For T2HK the numbers are $9\sigma$ to $3\sigma$ for both hierarchies. On the other hand, for 1.5° (2.5° and 2.0°) configurations of T2HKK, the sensitivity falls from $9\sigma$ to $7\sigma$ ($7\sigma$ to $4\sigma$) in NH and $10\sigma$ to $8\sigma$ ($7.5\sigma$ to $4.5\sigma$) in IH. From the plots we also see that the sensitivity of T2HK is better than the 2.0° and 2.5° configurations of T2HKK if the systematics is less than 2% and for NH the sensitivity of T2HK becomes comparable to the 1.5° off-axis configuration of T2HKK if the systematics is less than 1%. This is also one of the remarkable findings of our work. This also shows that if nature chooses the true hierarchy to be normal and $\delta_{CP} = -90°$, then T2HK is sufficient to determine the hierarchy sensitivity at a $5\sigma$ confidence level if the systematics is less than 3.5%. In these plots we also see that the curves corresponding to T2HK and DUNE are steeper than those for T2HKK. As explained earlier, because of the large number of event samples at the far detector, the effect of systematics is more for T2HK as compared to T2HKK, although both of their sensitivities lie around $4\sigma$ to $8\sigma$. On the other hand, the large variation in the sensitivity of DUNE with respect to the systematic errors is due to its large matter effect and higher hierarchy sensitivity as compared to T2HK and T2HKK.

In all the panels of Fig. 2, we see that among the three configurations of the T2HKK experiment, the hierarchy sensitivity is best for the 1.5° off-axis flux and as the detector is moved to higher off-axis angles, the sensitivity decreases. This is because the 1.5° off-axis flux covers more of the first oscillation maxima where the hierarchy sensitivity is maximum [20].

### C. Octant sensitivity

The octant sensitivity of an experiment is defined by its capability to rule out the wrong octant solution. In Fig. 3 we have given the octant sensitivity of T2HK, T2HKK, and DUNE as a function of the systematics. The upper panels are for the normal hierarchy and the lower panels are for the inverted hierarchy. In each row, the left panel corresponds to LO and the right panel corresponds to HO. The horizontal thin solid line corresponds to $5\sigma$ C.L. All the panels are for $\delta_{CP} = -90°$. Although we have shown our results for $\delta_{CP} = -90°$ only, we have checked that the conclusion remains the same for all the other values of $\delta_{CP}$.

For the lower octant (top left and bottom left panels) we see that if the systematics is less than 4% then the octant sensitivity of the T2HK experiment is better than all the other experiments. In this case the sensitivity of T2HK falls from $9\sigma$ to $4.5\sigma$ for both hierarchies as the systematics varies from 1% to 7%. The sensitivities of all three configurations of T2HKK are similar and the sensitivity falls from $7\sigma$ to $4.5\sigma$ for both hierarchies. Among all the experiments the sensitivity of DUNE is the lowest in NH and the sensitivity varies from $7\sigma$ to $4.5\sigma$ for both hierarchies. In these plots we see that the dependence of sensitivities on the systematic errors is similar for T2HKK and DUNE whereas the curves for T2HK are steeper than those for T2HKK and DUNE. This is because unlike the hierarchy sensitivity, the octant sensitivities of T2HKK and DUNE are similar. On the other hand due to the larger event sample of T2HK, the octant sensitivity of T2HK is greater than those of T2HKK and DUNE and thus more affected by the systematic uncertainties.

Now let us discuss the sensitivities for HO (top right and bottom right panels). In these case we see that except for T2HK in NH, the slopes of all the curves are almost equal. This can be understood in the following way. In general the octant sensitivity in HO is poorer than the LO as the denominator in the $\chi^2$ for HO is higher than LO. Thus it is natural that the effect of systematics will be less in HO as compared to LO. In this case the sensitivity of T2HK is the best among all the other setups for almost any value of the systematics in NH (thus more affected by systematics) and in IH the sensitivity of T2HK is the same as that of all three configurations of T2HKK and DUNE (thus the sensitivity of the all five setups depends similarly on systematics). Here the sensitivity falls from $6.5\sigma$ to $3\sigma$ for NH as the systematics varies from 1% to 7%. The dependence of the systematics for all three configurations of T2HKK is almost the same and they vary from 5% to 4% for both hierarchies. For NH, the sensitivity of DUNE is worse than all the other setups for any value of the systematics and it varies from $5\sigma$ to $3\sigma$.

## IV. RESULTS FOR NSI

In this section we will study the effect of the systematics error in constraining the NSI parameters. The nonstandard interaction in neutrino propagation can arise from the following four-fermion interaction:

$$\mathcal{L}_{\mathrm{eff}}^{\mathrm{NSI}} = -2\sqrt{2}\epsilon_{\alpha\beta}^{ff'P} G_F (\bar{\nu}_{\alpha L}\gamma_\mu \nu_{\beta L})(\bar{f}_P \gamma^\mu f'_P), \tag{7}$$

where $f_P$ and $f'_P$ correspond to fermions with chirality $P$, $\epsilon_{\alpha\beta}^{ff'P}$ is a dimensionless constant, and $G_F$ is the Fermi coupling constant. In the presence of NSI the MSW matter potential takes the following form:

$$\mathcal{A} \equiv \sqrt{2} G_F N_e \begin{pmatrix} 1+\epsilon_{ee} & \epsilon_{e\mu} & \epsilon_{e\tau} \\ \epsilon_{\mu e} & \epsilon_{\mu\mu} & \epsilon_{\mu\tau} \\ \epsilon_{\tau e} & \epsilon_{\tau\mu} & \epsilon_{\tau\tau} \end{pmatrix}, \tag{8}$$

where $\epsilon_{\alpha\beta}$ is defined by

$$\epsilon_{\alpha\beta} \equiv \sum_{f=e,u,d} \frac{N_f}{N_e} \epsilon_{\alpha\beta}^{f}. \tag{9}$$

$N_f (f = e, u, d)$ is the number densities of fermions $f$. Here we defined the NSI parameters as $\epsilon_{\alpha\beta}^{fP} \equiv \epsilon_{\alpha\beta}^{ffP}$ and $\epsilon_{\alpha\beta}^{f} \equiv \epsilon_{\alpha\beta}^{fL} + \epsilon_{\alpha\beta}^{fR}$. The present 90% bounds of the NSI parameters are given by [66,67]

$$\begin{pmatrix} |\epsilon_{ee}| < 4 \times 10^0 & |\epsilon_{e\mu}| < 3 \times 10^{-1} & |\epsilon_{e\tau}| < 3 \times 10^0 \\ & |\epsilon_{\mu\mu}| < 7 \times 10^{-2} & |\epsilon_{\mu\tau}| < 3 \times 10^{-1} \\ & & |\epsilon_{\tau\tau}| < 2 \times 10^1 \end{pmatrix}. \tag{10}$$

Thus we understand that the bounds on $\epsilon_{\alpha\mu}$ where $\alpha = e, \mu, \tau$ are stronger than the $\epsilon_{ee}$, $\epsilon_{e\tau}$, and $\epsilon_{\tau\tau}$. One additional bound comes from the high-energy atmospheric data which relates the parameters $\epsilon_{\tau\tau}$ and $\epsilon_{e\tau}$ as [68,69]

$$\epsilon_{\tau\tau} \simeq \frac{|\epsilon_{e\tau}|^2}{1+\epsilon_{ee}}. \tag{11}$$

In Ref. [70] it was shown that, in the high-energy behavior of the disappearance oscillation probability

$$\begin{aligned} 1 - P(\nu_\mu \to \nu_\mu) \\ \simeq c_0 + c_1 \frac{\Delta m_{31}^2/2E}{\sqrt{2} G_F N_e} + \mathcal{O}\left[\left(\frac{\Delta m_{31}^2/2E}{\sqrt{2} G_F N_e}\right)^2\right], \end{aligned} \tag{12}$$

in the presence of the matter potential (8), $|c_0| \ll 1$ and $|c_1| \ll 1$ imply that $|\epsilon_{e\mu}| \ll 1$, $|\epsilon_{\mu\mu}| \ll 1$, $|\epsilon_{\mu\tau}| \ll 1$, and $|\epsilon_{\tau\tau} - |\epsilon_{e\tau}|^2/(1+\epsilon_{ee})| \ll 1$. In deriving Eq. (12), it is assumed that $|1+\epsilon_{ee}|$ is not very small. $1+\epsilon_{ee} = 0$ is the abnormal region where the $e-e$ component of the matter effect vanishes [48], and the approximation (11) becomes invalid only in the neighborhood of $1+\epsilon_{ee} = 0$. As explained in Appendix A in Ref. [71], the region $1+\epsilon_{ee} = 0$ corresponds to the one $\epsilon_D = 1/6$ in the parametrization of the solar neutrino analysis [26]. The result in Ref. [26] shows that the region near $\epsilon_D = 1/6$ is excluded by the solar neutrino and KamLAND data at more than $3\sigma$.

The region in which the ansatz (11) may not be a good approximation is therefore excluded by the solar neutrino and KamLAND data, so Eq. (11) can be justified by implicitly assuming the prior from the analysis of the solar neutrino and KamLAND data.[3] Furthermore, from the Super-Kamiokande data [72], we get

$$\left|\frac{\epsilon_{e\tau}}{1+\epsilon_{ee}}\right| \lesssim 0.8 \quad \text{at } 3\sigma. \tag{13}$$

Keeping these facts in mind, we perform our analysis with the following ansatz:

$$\mathcal{A} = \sqrt{2}G_F N_e \begin{pmatrix} 1+\epsilon_{ee} & 0 & \epsilon_{e\tau} \\ 0 & 0 & 0 \\ \epsilon_{e\tau}^* & 0 & |\epsilon_{e\tau}|^2/(1+\epsilon_{ee}) \end{pmatrix}. \tag{14}$$

Thus the free parameters are $\epsilon_{ee}$, $|\epsilon_{e\tau}|$, and $\arg(\epsilon_{e\tau}) = \phi_{31}$.

Note that in our earlier work, we have studied the sensitivity of the T2HKK experiment to the nonstandard interactions in a similar fashion [49]. But at that time, the experimental details for the various T2HKK setups were not available and thus we have used the T2HK setup of [16] and scaled those events at 1100 km. But in the present analysis, we have used the configurations of the T2HKK as outlined in [17]. In the previous work the ratio of the neutrino and antineutrino run was 1∶1 but in the present analysis, we have taken the ratio to be 1∶3 following the T2HKK report. But the major difference of the present work as compared to the earlier work lies in the fact that here we have presented our results for four different sets of systematic errors, while in the previous work only one set of systematic errors was considered.

### A. Constraining the NSI parameters

In Fig. 4, we have plotted the sensitivity for the NSI parameters for different four values of the systematic errors in the $\epsilon_{ee}$ (test) vs $|\epsilon_{e\tau}|$ (test) plane. The true values of both the parameters are zero. Thus these plots describe the potential of these future beam-based experiments to put bounds on the NSI parameters. The true value of $\delta_{CP}$ is taken as $-90°$ and the true value of $\phi_{31}$ is zero. Both the parameters are marginalized over in the test. The true value of $\theta_{23}$ is 45° and this parameter is marginalized over in the test. The parameters $\theta_{13}$, $\theta_{12}$, $\Delta m^2_{21}$, and $\Delta m^2_{31}$ are kept fixed in both the true and test spectrums. Hierarchy is assumed to be known for these plots. The left (right) column of Fig. 4 corresponds to NH (IH). The first three rows correspond to the 2.5°, 2.0°, and 1.5° off-axis configurations of T2HKK, respectively, and the fourth row is for DUNE. In each panel the black solid curve corresponds to the bound $|\epsilon_{e\tau}/(1+\epsilon_{ee})| \lesssim 0.8$ at $3\sigma$.

From the figure we see that for the setups (OA 2.5, NH) and (OA 1.5, NH), the sensitivities corresponding to the 1% and 3% systematic uncertainties are similar as are the sensitivities corresponding to 5% and 7%. An improvement of the systematics from 5% to 3% improves the sensitivity significantly. For (OA 2.5, IH) the sensitivity for all four cases of the systematic uncertainties are similar. Thus in this case the systematic uncertainties do not play a significant role. For (OA 2.0, NH) and (DUNE, NH) the sensitivity for the NSI parameters gets improved as the systematics errors are lowered from 7% to 1%. For (OA 2.0, IH); (OA 1.5, IH); and (DUNE, IH), the sensitivities corresponding to the 1%, 3%, and 5% systematic errors are similar. Among the three setups of the T2HKK experiment, the configuration with 1.5° off-axis flux covers a maximum area in the probability spectrum in the higher energy region and the configuration with 2.5° covers the minimum area in the probability spectrum in the lower energy region. For this reason the 1.5° off-axis configuration has the maximum capability of constraining the NSI parameters and the 2.5° off-axis configuration has the minimum capability. For a similar reason, the effect of systematics in the 1.5° off-axis configuration is greater compared to the other two setups of T2HKK.

### B. Constraining the *CP* phases

In Fig. 5, we have plotted the 90% C.L. contours in the $\delta_{CP}$ (test)—$\phi_{31}$ (test) plane for four values of the systematic errors for true values of $\delta_{CP} = -90°$ and $\phi_{31} = 0°$. For these plots we have considered the true values of $\epsilon_{ee} = 0.8$ and $|\epsilon_{e\tau}| = 0.2$ and they are marginalized over in the test. Thus these figures correspond to the capability of these future long-baseline experiments to constrain the *CP* phases, assuming NSI exist in nature. The parameter $\theta_{23}$ is 45° in the true spectrum and marginalized over in the test. As for the earlier case $\theta_{13}$, $\theta_{12}$, $\Delta m^2_{21}$, and $\Delta m^2_{31}$ are kept fixed in both the true and test spectrums. Hierarchy is assumed to be known in all the panels. The left column is for NH and the right column is for IH. The first three rows correspond to the 2.5°, 2.0°, and 1.5° off-axis configurations of T2HKK, respectively. The fourth row is for DUNE. In each panel the "+" symbol signifies the true values of $\delta_{CP}$ and $\phi_{31}$.

From the plots we see the following. For the setups (OA 2.5, NH); (OA 1.5, NH); and (OA 1.5, IH), the sensitivities corresponding to the 1% and 3% systematic errors are similar so the sensitivities of 5% and 7%. A reduction of the systematics from 5% to 3% causes a significant improvement in the sensitivity. For the setup (OA 2.5, IH), the systematic uncertainties do not play any role for the

[3] In Ref. [72] is was concluded that the best-fit point in the $(\epsilon_{ee}, |\epsilon_{e\tau}|)$ plane is given by $(-1.0, 0.0)$ using the Super-Kamiokande atmospheric neutrino data for 4438 days. However, the allowed region within $2\sigma$ is quite wide in the result of Ref. [72] because the analysis is based on the energy rate only, as the energy spectrum information is not available. Hence the best-fit value $(\epsilon_{ee}, |\epsilon_{e\tau}|) = (-1.0, 0.0)$ is only a qualitative estimate.

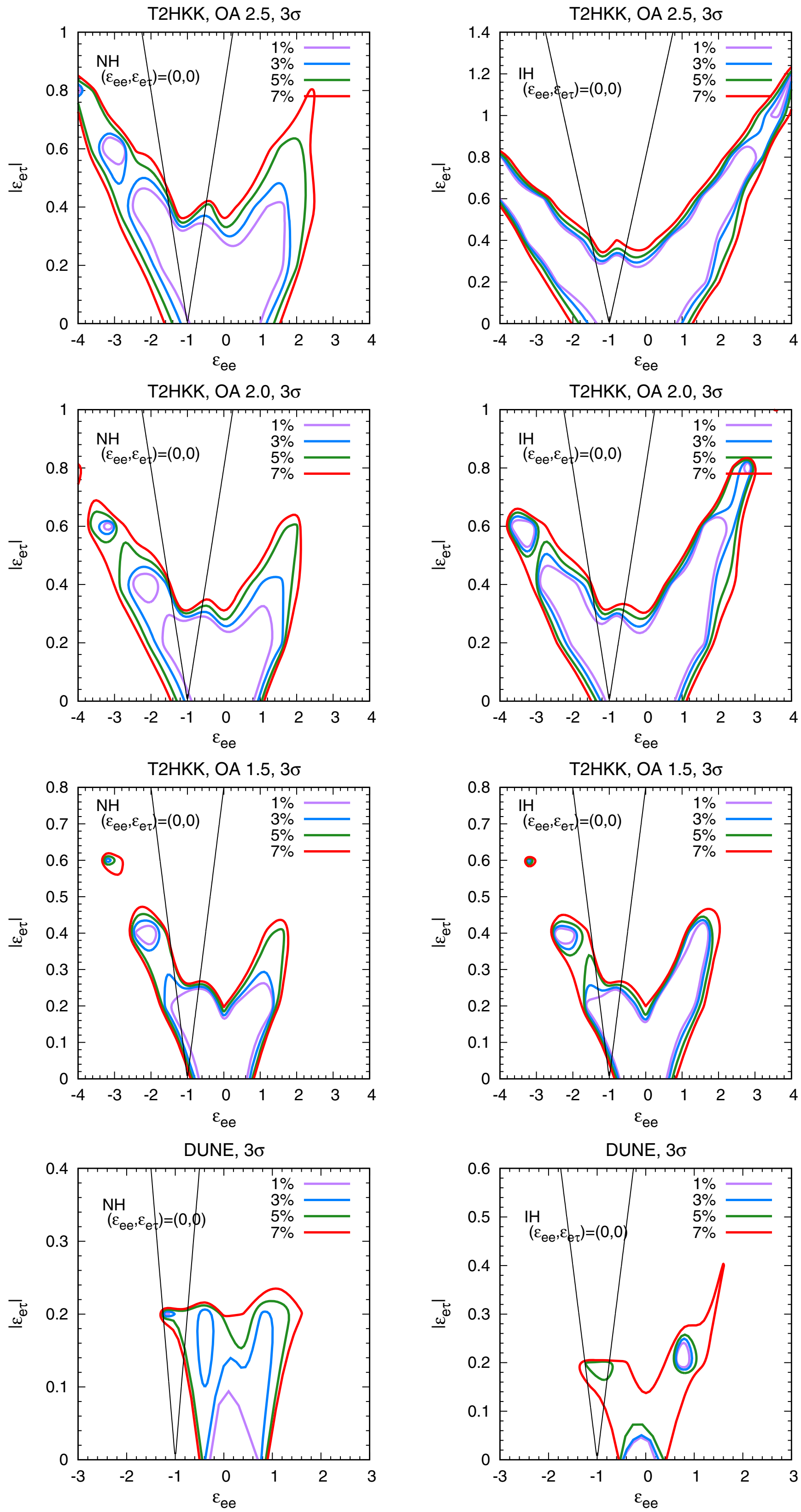


FIG. 4. Sensitivity for NSI parameters for four values of the systematic errors. The left column is for NH and the right column is for IH. The thin solid diagonal straight line stands for the bound $|\tan\beta| = |\epsilon_{e\tau}/(1+\epsilon_{ee})| \lesssim 0.8$ [72] at $3\sigma$ from the current atmospheric data by Super-Kamiokande. The first three rows correspond to the 2.5°, 2.0°, and 1.5° off-axis configurations for T2HKK, respectively. The fourth row is for DUNE.

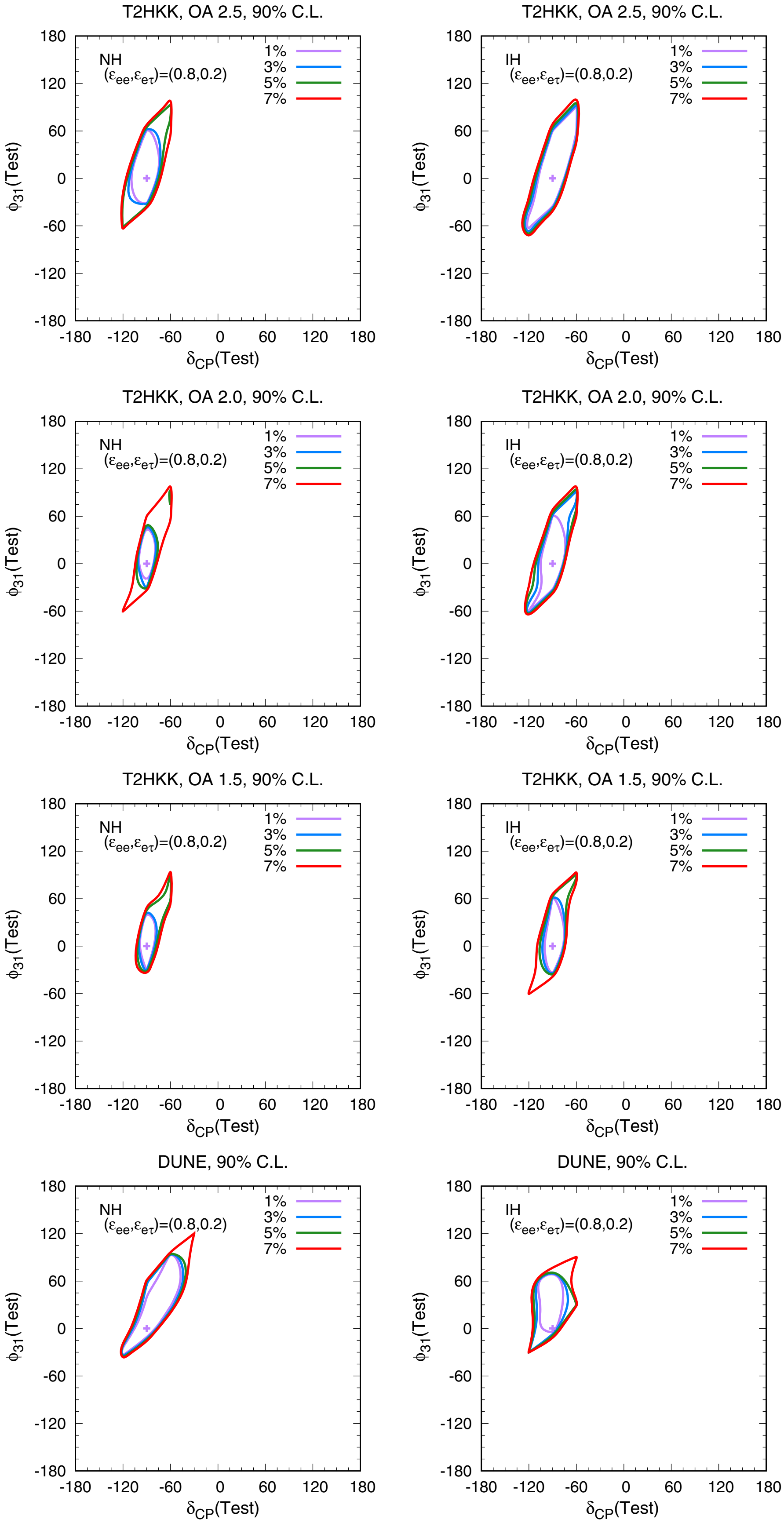


FIG. 5. Sensitivity to the *CP* phases for four values of the systematic errors. The left column is for NH and the right column is for IH. The first three rows correspond to the 2.5°, 2.0°, and 1.5° off-axis configurations for T2HKK, respectively. The fourth row is for DUNE.

sensitivity as the result is similar for all four values of the systematic errors. For (OA 2.0, NH); (DUNE, NH); and (DUNE, IH), the sensitivity is similar for the systematic uncertainties of 1%, 3%, and 5%. On the other hand for the setup (OA 2.0, IH), the sensitivities corresponding to 3%, 5%, and 7% are quite similar. As explained earlier, the capability of the 1.5° off-axis configuration in constraining the *CP* phases is better among the other two setups of T2HKK.

## V. CONCLUSION

In this paper we have done a comparative study of T2HK, T2HKK, and DUNE in the standard three-flavor scenario and the case with new physics with respect to the systematic errors. In the standard oscillation case we have studied the effect of the systematics in determining the unknowns in the neutrino oscillation sector, i.e., neutrino mass hierarchy, octant of the mixing angle $\theta_{23}$, and *CP* violation. As a probe of new physics we have analyzed the role of the systematic uncertainties in constraining the parameters of the nonstandard interactions in the neutrino propagation. In our analysis we have taken four pull variables, which are (i) signal normalization, (ii) background normalization, (iii) signal tilt, and (iv) background tilt. We have fixed the tilt errors to a constant value and presented our results as a function of the normalization errors. The normalization errors corresponding to signal and background are considered to be equal to each other in our treatment. Note that our method of incorporating the systematic errors is quite simplistic in the sense that instead of considering the pull variables for each source of systematics as in [17], we have considered a single pull variable corresponding to an overall normalization factor. But still the results discussed in this work provide useful guidance on how the sensitivity of various experiments may depend on the achieved systematic uncertainties. We find that the variation of the sensitivity with respect to the systematic errors depends on the nature of the true parameter space. For a given set of the true parameters, if the sensitivity of a particular experiment is very high, then its sensitivity varies much more with respect to their systematic errors. Our results also show that the variation of the sensitivity of the T2HK experiment is larger compared to that for the T2HKK setup in the standard oscillation scenario. The major findings of our work are as follows: (i) If the hierarchy is known, then T2HK can have the best CPV discovery sensitivity among all the setups considered in this analysis if the systematics is reduced to within 1%. The CPV discovery potential of T2HK is poor because of the lack of information of the mass hierarchy/matter effect. On the other hand, placing a detector at a longer distance may affect the *CP* sensitivity because of the reduction in statistics. Thus, if the information of the mass hierarchy comes from a different experiment like DUNE, then our results establish the fact that placing both the detectors at 295 km can give a better *CP* sensitivity than keeping one detector at 295 km and the other at 1100 km, if the systematics are reduced to 1%. (ii) For the favorable combinations of the true hierarchy and the true $\delta_{CP}$, the hierarchy sensitivity of T2HK will be comparable to the 1.5° off-axis configuration of T2HKK if the systematics is 1% and the true hierarchy is normal. But among all the setups, the best hierarchy sensitivity will come for DUNE for any value of systematic errors for this favorable parameter space. For the unfavorable parameter space, the hierarchy sensitivities are almost constant when the systematic error is varied, but still the best sensitivity comes from the DUNE experiment. (iii) Regarding the octant sensitivity, we find that if nature chooses the lower octant, then T2HK will give the best octant sensitivity among all the setups if the systematic error is less than 4% and in the case of the true higher octant, the sensitivity of T2HK is always the best for all the values of the systematics for NH. On the other hand, in the study of the dependence of the sensitivity to the NSI parameters on systematic errors, we find that different setups respond differently for various values of systematic errors. Our major findings are as follows: (i) Apart from the 2.0° off-axis configuration in IH, i.e., (OA 2.0, IH), capabilities of all the setups are sensitive to systematic errors. (ii) The capability of (OA 2.0, NH) and (DUNE, NH) in constraining $\epsilon_{ee}$ and $|\epsilon_{e\tau}|$ gets chronologically improved as the systematics is reduced from 7% to 1%. (iii) For the other setups, the sensitivities corresponding to the 1% and 3% systematics errors are similar in constraining $\epsilon_{ee}$ and $|\epsilon_{e\tau}|$. (iv) In constraining the *CP* phases, except (OA 2.0, IH), lowering systematic uncertainty below 3% would not result in a significant improvement in the achieved sensitivity. Thus from the above discussion, we understand that measurement of the systematics plays an important role in the sensitivity reach of the future high statistics long-baseline experiments. Depending on the value of the systematics, the sensitivity of one experiment can be better than others. Thus the results shown in this work can serve as guidance for much more realistic studies by experimental groups in planning the future generation long-baseline experiments.

## ACKNOWLEDGMENTS

M. G. would like to thank Srubabati Goswami for useful discussions. M. G. also thanks Kaustav Chakraborty for useful discussions on GLoBES. This research was partly supported by a Grant-in-Aid for Scientific Research of the Ministry of Education, Science and Culture, under Grants No. 25105009, No. 15K05058, No. 25105001, and No. 15 K21734.

[1] L. Magaletti, Proc. sci. NOW2016 (**2016**) 003.
[2] P. Vahle (2016), Proceedings at Neutrino 2016, London.
[3] P. Adamson *et al.* (NOvA Collaboration), Phys. Rev. Lett. **118**, 151802 (2017).
[4] S. Prakash, S. K. Raut, and S. U. Sankar, Phys. Rev. D **86**, 033012 (2012).
[5] S. K. Agarwalla, S. Prakash, and S. U. Sankar, J. High Energy Phys. 07 (2013) 131.
[6] V. Barger, D. Marfatia, and K. Whisnant, Phys. Rev. D **65**, 073023 (2002).
[7] M. Ghosh, P. Ghoshal, S. Goswami, N. Nath, and S. K. Raut, Phys. Rev. D **93**, 013013 (2016).
[8] A. Ghosh, T. Thakore, and S. Choubey, J. High Energy Phys. 04 (2013) 009.
[9] M. Ghosh, P. Ghoshal, S. Goswami, and S. K. Raut, Phys. Rev. D **89**, 011301 (2014).
[10] S. Prakash, U. Rahaman, and S. U. Sankar, J. High Energy Phys. 07 (2014) 070.
[11] M. Ghosh, P. Ghoshal, S. Goswami, and S. K. Raut, Nucl. Phys. **B884**, 274 (2014).
[12] A. Chatterjee, P. Ghoshal, S. Goswami, and S. K. Raut, J. High Energy Phys. 06 (2013) 010.
[13] M. Ghosh, Phys. Rev. D **93**, 073003 (2016).
[14] S. Bharti, S. Prakash, U. Rahaman, and S. U. Sankar, arXiv:1602.03513.
[15] C. Soumya and R. Mohanta, Eur. Phys. J. C **76**, 302 (2016).
[16] K. Abe *et al.* (Hyper-Kamiokande Working Group), arXiv:1412.4673.
[17] K. Abe *et al.* (Hyper-Kamiokande Proto-Collaboration), arXiv:1611.06118.
[18] R. Acciarri *et al.* (DUNE Collaboration), arXiv:1512.06148.
[19] S. Fukasawa, M. Ghosh, and O. Yasuda, Nucl. Phys. **B918**, 337 (2017).
[20] P. Ballett, S. F. King, S. Pascoli, N. W. Prouse, and T. Wang, arXiv:1612.07275.
[21] L. Wolfenstein, Phys. Rev. D **17**, 2369 (1978).
[22] M. M. Guzzo, A. Masiero, and S. T. Petcov, Phys. Lett. B **260**, 154 (1991).
[23] E. Roulet, Phys. Rev. D **44**, R935 (1991).
[24] T. Ohlsson, Rep. Prog. Phys. **76**, 044201 (2013).
[25] O. G. Miranda and H. Nunokawa, New J. Phys. **17**, 095002 (2015).
[26] M. C. Gonzalez-Garcia and M. Maltoni, J. High Energy Phys. 09 (2013) 152.
[27] A. Friedland and I. M. Shoemaker, J. Phys. G **43**, 095005 (2016).
[28] R. Adhikari, S. Chakraborty, A. Dasgupta, and S. Roy, Phys. Rev. D **86**, 073010 (2012).
[29] M. Masud, A. Chatterjee, and P. Mehta, J. Phys. G **43**, 095005 (2016).
[30] A. de Gouva and K. J. Kelly, Nucl. Phys. **B908**, 318 (2016).
[31] Z. Rahman, A. Dasgupta, and R. Adhikari, J. Phys. G **42**, 065001 (2015).
[32] P. Coloma, J. High Energy Phys. 03 (2016) 016.
[33] J. Liao, D. Marfatia, and K. Whisnant, Phys. Rev. D **93**, 093016 (2016).
[34] C. Soumya and R. Mohanta, Phys. Rev. D **94**, 053008 (2016).
[35] M. Blennow, S. Choubey, T. Ohlsson, D. Pramanik, and S. K. Raut, J. High Energy Phys. 08 (2016) 090.
[36] D. V. Forero and P. Huber, Phys. Rev. Lett. **117**, 031801 (2016).
[37] K. Huitu, T. J. Krkkinen, J. Maalampi, and S. Vihonen, Phys. Rev. D **93**, 053016 (2016).
[38] P. Bakhti and Y. Farzan, J. High Energy Phys. 07 (2016) 109.
[39] M. Masud and P. Mehta, Phys. Rev. D **94**, 013014 (2016).
[40] P. Coloma and T. Schwetz, Phys. Rev. D **94**, 055005 (2016).
[41] M. Masud and P. Mehta, Phys. Rev. D **94**, 053007 (2016).
[42] S. K. Agarwalla, S. S. Chatterjee, and A. Palazzo, Phys. Lett. B **762**, 64 (2016).
[43] S.-F. Ge and A. Yu. Smirnov, J. High Energy Phys. 10 (2016) 138.
[44] J. Liao, D. Marfatia, and K. Whisnant, Phys. Lett. B **767**, 350 (2017).
[45] S. Fukasawa, M. Ghosh, and O. Yasuda, arXiv:1609.04204.
[46] M. Blennow, P. Coloma, E. Fernandez-Martinez, J. Hernandez-Garcia, and J. Lopez-Pavon, J. High Energy Phys. 04 (2017) 153.
[47] J. Liao, D. Marfatia, and K. Whisnant, J. High Energy Phys. 01 (2017) 071.
[48] K. N. Deepthi, S. Goswami, and N. Nath, arXiv: 1612.00784.
[49] S. Fukasawa, M. Ghosh, and O. Yasuda, Phys. Rev. D **95**, 055005 (2017).
[50] P. Huber, M. Lindner, and W. Winter, Nucl. Phys. **B645**, 3 (2002).
[51] T. Ohlsson and W. Winter, Phys. Rev. D **68**, 073007 (2003).
[52] V. Barger, P. Huber, D. Marfatia, and W. Winter, Phys. Rev. D **76**, 053005 (2007).
[53] P. Huber, M. Mezzetto, and T. Schwetz, J. High Energy Phys. 03 (2008) 021.
[54] P. Coloma and E. Fernandez-Martinez, J. High Energy Phys. 04 (2012) 089.
[55] J. Tang and W. Winter, Phys. Rev. D **80**, 053001 (2009).
[56] A. M. Ankowski and C. Mariani, J. Phys. G **44**, 054001 (2017).
[57] P. Coloma, P. Huber, J. Kopp, and W. Winter, Phys. Rev. D **87**, 033004 (2013).
[58] P. Huber, M. Lindner, and W. Winter, Comput. Phys. Commun. **167**, 195 (2005).
[59] P. Huber, J. Kopp, M. Lindner, M. Rolinec, and W. Winter, Comput. Phys. Commun. **177**, 432 (2007).
[60] M. Blennow and E. Fernandez-Martinez, Comput. Phys. Commun. **181**, 227 (2010).
[61] D. V. Forero, M. Tortola, and J. W. F. Valle, Phys. Rev. D **90**, 093006 (2014).
[62] I. Esteban, M. C. Gonzalez-Garcia, M. Maltoni, I. Martinez-Soler, and T. Schwetz, J. High Energy Phys. 01 (2017) 087.
[63] F. Capozzi, G. L. Fogli, E. Lisi, A. Marrone, D. Montanino, and A. Palazzo, Phys. Rev. D **89**, 093018 (2014).
[64] H. Nunokawa, S. J. Parke, and R. Zukanovich Funchal, Phys. Rev. D **72**, 013009 (2005).
[65] S. K. Raut, Mod. Phys. Lett. A **28**, 1350093 (2013).

[66] S. Davidson, C. Pena-Garay, N. Rius, and A. Santamaria, J. High Energy Phys. 03 (2003) 011.

[67] C. Biggio, M. Blennow, and E. Fernandez-Martinez, J. High Energy Phys. 08 (2009) 090.

[68] A. Friedland, C. Lunardini, and M. Maltoni, Phys. Rev. D **70**, 111301 (2004).

[69] A. Friedland and C. Lunardini, Phys. Rev. D **72**, 053009 (2005).

[70] H. Oki and O. Yasuda, Phys. Rev. D **82**, 073009 (2010).

[71] S. Fukasawa and O. Yasuda, Nucl. Phys. **B914**, 99 (2017).

[72] S. Fukasawa and O. Yasuda, Adv. High Energy Phys. **2015**, 820941 (2015).